Supplementary Information

Applied machine learning for prediction of CO_2 adsorption on biomass waste-derived porous carbons

*Xiangzhou Yuan [a,b,§], Manu Suvarna [c,§], Sean Low [c], Pavani Dulanja Dissanayake [a], Ki Bong Lee [d], Jie Li [c], Xiaonan Wang [c,**], Yong Sik Ok [a,*]*

[a] Korea Biochar Research Center, APRU Sustainable Waste Management Program & Division of Environmental Science and Ecological Engineering, Korea University, Seoul 02841, Republic of Korea

[b] R&D Centre, Sun Brand Industrial Inc., Jeollanam-do, 57248, Republic of Korea

[c] Department of Chemical and Biomolecular Engineering, National University of Singapore, Singapore 117585, Singapore

[d] Department of Chemical & Biological Engineering, Korea University, Seoul 02841, Republic of Korea

[§] These authors contributed equally to this work.

[*] Corresponding author: Email: yongsikok@korea.ac.kr (Y.S. Ok)

[**] Corresponding author: Email: chewxia@nus.edu.sg (X. Wang)

Summary:

No. of pages: 67; No. of figures: 1; No. of tables: 4

Table S1. Biomass waste-derived porous carbons (BWDPCs) without heteroatom-doping treatment.

Carbon precursors	Upcycling for porous carbons			Textural properties			Ultimate analysis (%)				CO_2 uptake (mmol/g)		
	Carbonization	**Activation**	**Activation**	**S_{BET} [a] (m^2/g)**	**V_{toal} [b] (cm^3/g)**	**V_{micro} [c] (cm^3/g)**	**C**	**H**	**N**	**O [*]**	**25 °C and 1 bar**	**0 °C and 1 bar**	**25 °C and 0.15 bar**
Wood chip [1]	10 kW fixed-bed, downdraft gasification (800–1000 °C)	KOH activation at 850 °C for 2 h		1,281.6	0.71	0.32	69.22	3.99	0.08	26.30	2.63		
		KOH activation at 850 °C for 2 h	CO_2 activation at 550 °C for 1 h	1,012.6	0.56	0.22	64.83	3.64	0.38	30.77	2.59		
70% wood chips and 30% chicken manure [1]		KOH activation at 850 °C for 2 h		1,408.8	0.83	0.36	72.41	3.63	0.01	23.59	2.92		
		KOH activation at 850 °C for 2 h	CO_2 activation at 550 °C for 1 h	1,403.9	0.85	0.33	69.51	4.35	0.76	24.94	2.44		
40% food waste + 60% wood [2]		KOH activation at 850 °C for 2 h		841.3	0.36						3.23		

		KOH activation at 850 °C for 2 h	CO_2 activation at 550 °C for 1 h	667.4	0.29						2.73		
Spent coffee ground [3]		K_2CO_3 activation at 600 °C for 1 h		645	0.26	0.25	70.86	1.71	3.19	14.72	3.45		1.43
		K_2CO_3 activation at 600 °C for 5 h		750	0.30	0.29	83.88	1.63	3.27	5.30	3.65		1.46
		K_2CO_3 activation at 700 °C for 1 h		1,259	0.52	0.49	87.56	1.06	1.87	0.23	4.33		1.36
		K_2CO_3 activation at 700 °C for 5 h		1,476	0.61	0.60	91.62	0.80	1.67	0.00	4.54		1.30
		K_2CO_3 activation at 800 °C for 1 h		1,692	0.71	0.68	94.51	0.58	1.51	0.00	4.46		1.20
		K_2CO_3 activation at 800 °C for 5 h		2,337	1.15	0.85	82.66	0.59	1.55	0.00	3.78		0.92
Potato starch [4]	Hydrothermal carbonization at 180 °C for 12 h	600 °C for 1 h		1,409	0.69	0.51							0.70§
			1000 °C for 10 min with Air	1,340	0.66	0.49							0.85§
Onion peel [5]	500 °C for 1 h			5.4	0.00						0.74§		
	600 °C for 1 h			207	0.16						1.43§		
	700 °C for 1 h			550	0.37						1.68§		
	800 °C for 1 h			692	0.43						1.59§		

	900 °C for 1 h			930	0.54						1.57[§]		
Pine sawdust [6]	700 °C for 2 h	KOH activation at 700 °C for 2 h		1,728.66	0.70	0.67	93.40	0.73	0.89	6.79	4.21		
	700 °C for 2 h	KOH activation at 800 °C for 2 h		2,279.52	0.99	0.91	96.96	0.18	0.99	4.51	3.46		
	700 °C for 2 h	KOH activation at 900 °C for 2 h		2,330.89	1.91	0.98	87.57	0.17	1.30	7.35	2.45		
Date [7]	500 °C for 2 h	KOH (2) activation at 800 °C for 1 h		2,112	0.94	0.86					4.18		
	500 °C for 2 h	KOH (4) activation at 800 °C for 1 h		3,255	1.65	1.29					3.35		
	500 °C for 2 h	KOH (6) activation at 800 °C for 1 h		3,337	2.05	0.54					2.90		
	800 °C for 2 h	KOH (2) activation at 800 °C for 1 h		1,634	0.76	0.56					4.14		
	800 °C for 2 h	KOH (4) activation at 800 °C for 1 h		2,367	1.15	0.83					4.36		
	800 °C for 2 h	KOH (6) activation at 800 °C for 1 h		2,844	1.63	0.89					3.65		
Bee-collected pollen [8]	800 °C for 4 h	KOH (1:3) activation at 800 °C for 2 h		232	0.11	0.09	80.82		2.34	15.36	1.77		0.98

	800 °C for 4 h	KOH (1:2) activation at 800 °C for 2 h		332	0.16	0.12	76.25		1.89	21.86	2.10		1.04
	800 °C for 4 h	KOH (1:1) activation at 800 °C for 2 h		937	0.40	0.38	77.57		1.54	20.89	3.38		1.18
	800 °C for 4 h	KOH (2:1) activation at 800 °C for 2 h		1,214	0.53	0.48	79.37		1.18	19.45	3.40		0.85
	800 °C for 4 h	KOH (3:1) activation at 800 °C for 2 h		1,460	0.63	0.53	93.10		0.31	6.59	3.42		0.69
Garlic peel [9]	360 °C for 2 h	KOH (1:1) activation at 700 °C for 1 h		1,049	0.69	0.43					3.80		
	360 °C for 2 h	KOH (2:1) activation at 700 °C for 1 h		1,248	0.68	0.52					4.10		
Biomass tar [10]		CaO/KOH (1:1) activation at 300 °C for 1 h	CaO/KOH activation at 800 °C for 1 h	1,898	1.52	0.43					2.44	3.81	0.80

		CaO/KOH (1:2) activation at 300 °C for 1 h	CaO/KOH activation at 800 °C for 1 h	1,790	1.21	0.48					2.71	4.40	0.74
		CaO/KOH (1:3) activation at 300 °C for 1 h	CaO/KOH activation at 800 °C for 1 h	2,424	1.38	0.51					2.67	4.10	0.70
		CaO/KOH (2:2) activation at 300 °C for 1 h	CaO/KOH activation at 800 °C for 1 h	2,358	1.85	0.49					2.92	4.77	1.01
		CaO/KOH (2:3) activation at 300 °C for 1 h	CaO/KOH activation at 800 °C for 1 h	1,829	1.25	0.49					3.13	5.03	1.20
		CaO/KOH (2:4) activation at 300 °C for 1 h	CaO/KOH activation at 800 °C for 1 h	1,684	1.43	0.48					2.75	4.62	0.68
Biomass tar [11]		KOH (0.5) activation at 300 °C for 0.5 h	KOH activation at 600 °C for 0.5 h	660	0.28	0.24	83.48		3.53	12.98	2.94	4.22	0.74

		KOH (0.5) activation at 300 °C for 0.5 h	KOH activation at 700 °C for 0.5 h	1,076	0.44	0.38	84.57		3.03	9.46	4.11	6.02	1.64
		KOH (0.5) activation at 300 °C for 0.5 h	KOH activation at 800 °C for 0.5 h	1,268	0.55	0.50	90.49		2.12	7.39	3.64	5.43	1.22
		KOH (0.5) activation at 300 °C for 0.5 h	KOH activation at 900 °C for 0.5 h	1,480	0.71	0.48	89.42		2.08	7.04	3.31	5.41	1.52
		KOH (0.25) activation at 300 °C for 0.5 h	KOH activation at 700 °C for 0.5 h	1,161	0.38	0.35	88.44		3.02	8.53	3.69	5.82	1.38
		KOH (1.0) activation at 300 °C for 0.5 h	KOH activation at 700 °C for 0.5 h	1,804	0.85	0.66	89.93		2.00	8.07	3.16	5.20	0.96
		KOH (2.0) activation at 300 °C for 0.5 h	KOH activation at 700 °C for 0.5 h	1,857	0.87	0.48	92.01		1.32	6.67	3.06	5.04	0.92

Glucose [12]	180 °C for 10 h	KOH activation at 500 °C for 1 h		972	0.49	0.39				14.24	3.01	4.33	0.95
		KOH activation at 600 °C for 1 h		1,515	0.90	0.62				11.18	4.19	6.38	1.18
		KOH activation at 700 °C for 1 h		1,815	1.02	0.74				11.26	3.91	6.25	0.87
		KOH activation at 800 °C for 1 h		2,305	1.12	0.93				7.83	3.96	6.99	0.93
Banana stems [13]	700 °C for 2 h			909	0.44	0.32	79.50	1.50		19.00	3.20	5.30	
Banana fiber [13]				1,260	0.81	0.56	84.00	2.00		14.00	5.00	7.10	
Flesh from sunflower receptacle [14]	500 °C for 2 h	KOH activation at 800 °C for 2 h		3,072	1.77	0.78	91.02	2.71	0.40	5.87	2.78	4.09	
Flesh from sunflower stalk [14]	500 °C for 2 h	KOH activation at 800 °C for 2 h		2,730	1.84	1.12	94.50	0.95	0.80	3.75	2.34	4.08	
	1000 °C for 1 h			654	0.46	0.36	77.12	1.08	0.75	21.05	3.08	4.52	
Cellulose fibers [15]		Steam activation at 650 °C for 2 h		473	0.20	0.17	88.40	2.20	0.00	9.40	1.72		0.70
		Steam activation at 700 °C for 2 h		593	0.25	0.21	83.70	0.60	0.00	15.70	2.33		0.90
P.nigra wood [15]		Steam activation at 600 °C for 2 h		217	0.12	0.13	89.60	2.60	1.00	6.80	1.12		0.50
Camphor leaves [16]	500 °C for 2 h	KOH activation at 500 °C for 1 h		721	0.35	0.29			3.00		2.77	4.50	

		KOH activation at 600 °C for 1 h		1,146	0.55	0.47			1.50		3.74	5.86	
		KOH activation at 700 °C for 1 h		1,446	0.68	0.49			0.80		2.81	5.26	
		KOH activation at 800 °C for 1 h		1,736	0.87	0.36			0.70		2.42	4.80	
Corn stover [17]	250 °C for 10 h	KOH (2:2) activation at 600 °C for 2 h		955	0.43	0.31	57.46	3.37	0.66			4.93	
		KOH (2:2) activation at 700 °C for 2 h		1,539	0.72	0.48	59.20	3.70	0.34			6.80	
		KOH (2:2) activation at 800 °C for 2 h		2,442	1.56	0.86	60.41	3.91	0.24			7.14	
		KOH (2:2) activation at 900 °C for 2 h		2,225	1.11	0.49	64.90	3.12	0.24			5.79	
		KOH (1:2) activation at 800 °C for 2 h		1,543	0.71	0.61	66.56	2.99	0.86			5.06	
		KOH (3:2) activation at 800 °C for 2 h		2,201	1.31	0.69	56.55	3.03	0.31			6.22	

		KOH (4:2) activation at 800 °C for 2 h		2,170	1.27	0.66	54.94	2.19	0.32			4.86	
		KOH (2:1) activation at 800 °C for 2 h		1,630	0.69	0.60	76.91	2.73	0.20			6.47	
		KOH (2:3) activation at 800 °C for 2 h		2,132	1.13	0.70	59.22	3.88	0.23			6.85	
		KOH (2:4) activation at 800 °C for 2 h		1,862	0.81	0.69	58.22	3.79	0.22			6.32	
Stem of Arundo donax [18]		KOH (1) activation at 600 °C for 1 h		637	0.35	0.25						4.00	
		KOH (2) activation at 600 °C for 1 h		1,122	0.59	0.50						6.30	
		KOH (3) activation at 600 °C for 1 h		849	0.50	0.31						3.70	
Fresh cauliflower [19]	600 °C for 3 h			1,019	0.71	0.10					2.40		
	800 °C for 3 h			1,107	0.79	0.13					2.70		
	1000 °C for 3 h			1,139	1.26	0.24					3.10		

Lotus stem [20]	180 °C for 24 h	450 °C for 2 h	KOH activation at 800 °C for 1 h (char/KOH = 1:2)	2,091	0.87	0.65					3.85	6.17	
		450 °C for 2 h	KOH activation at 800 °C for 1 h (char/KOH = 1:4)	2,893	1.59	0.70					2.84	4.61	
Sawdust [21]	400 °C for 1 h	KOH (2) activation at 600 °C for 1 h		1,511	0.65	0.54	78.20	1.90		19.90	4.30		1.20
		KOH (2) activation at 700 °C for 1 h		1,830	0.78	0.67	83.40	0.90		15.70	4.90		1.10
		KOH (2) activation at 800 °C for 1 h		2,163	0.93	0.74	88.10	0.40		11.50	4.70		1.10
		KOH (4) activation at 800 °C for 1 h		2,610	1.15	0.74	88.70	0.40		10.90	4.00		0.90
Vine shoot [22]	600 °C for 1 h	CO_2 (0.1) activation at 600 °C		2.48								2.18	1.18$^{\psi}$
		CO_2 (1) activation at 600 °C		46.3								2.21	1.20$^{\psi}$
		CO_2 (0.1) activation at 800 °C		374	0.19	0.11						3.45	1.68$^{\psi}$

		KOH (2) activation at 600 °C		538	0.24	0.18						3.19	1.76$^{\psi}$
		KOH (2) activation at 700 °C		1,032	0.49	0.35						4.38	1.92$^{\psi}$
		KOH (5) activation at 600 °C		864	0.41	0.28						3.74	1.78$^{\psi}$
		KOH (5) activation at 700 °C		1,439	0.67	0.49						6.08	2.27$^{\psi}$
		KOH (1) activation at 600 °C		704	0.29	0.24						4.16	2.16$^{\psi}$
		KOH (1) activation at 600 °C		1,101	0.54	0.38						5.36	2.42$^{\psi}$
		KOH (2) activation at 600 °C		1,305	0.53	0.45						6.04	2.25$^{\psi}$
		KOH (2) activation at 700 °C		1,671	0.67	0.59						5.40	2.25$^{\psi}$
Pomegranate peel [23]		KOH activation at 700 °C for 1 h		585	0.28	0.20					4.11	6.03	
Carrot peel [23]				1,379	0.58	0.51					4.18	5.64	
Fern leaves [23]				1,593	0.74	0.54					4.12	4.52	
Jujun grass [24]	250 °C for 2 h	KOH (2) activation at 600 °C for 1 h		1,048	0.51	0.43					4.30		1.50
		KOH (2) activation at 700 °C for 1 h		1,512	0.74	0.62					4.90		1.50

		KOH (2) activation at 800 °C for 1 h		2,735	1.47	0.94					3.80		0.90
		KOH (4) activation at 600 °C for 1 h		2,396	1.15	0.96					3.50		0.90
		KOH (4) activation at 700 °C for 1 h		3,144	1.56	1.23					4.10		0.90
		KOH (4) activation at 800 °C for 1 h		2,957	1.72	0.75					2.80		0.60
Camellia japonica [24]		KOH (2) activation at 600 °C for 1 h		1,150	0.56	0.47					4.70		1.50
		KOH (2) activation at 700 °C for 1 h		1,353	0.67	0.56					5.00		1.50
		KOH (2) activation at 800 °C for 1 h		1,917	0.99	0.75					3.70		0.90
		KOH (4) activation at 600 °C for 1 h		2,345	1.20	0.89					3.10		0.80
		KOH (4) activation at 700 °C for 1 h		2,983	1.50	1.14					3.00		0.70
		KOH (4) activation at 800 °C for 1 h		3,537	1.85	1.21					2.80		0.60
Empty fruit bunch [25]	150 °C for 20 min	KOH activation at 600 °C for 0.5 h		1,163	0.23	0.10					0.66		
	250 °C for 20 min	KOH activation at 600 °C for 0.5 h		2,239	0.88	0.19					0.85		

	350 °C for 20 min	KOH activation at 600 °C for 0.5 h		1,720	0.56	0.15					2.81		
	150 °C for 20 min	KOH activation at 800 °C for 0.5 h		1,322	0.78	0.23					3.40		
	250 °C for 20 min	KOH activation at 800 °C for 0.5 h		2,510	1.05	0.55					3.71		
	350 °C for 20 min	KOH activation at 800 °C for 0.5 h		2,100	0.78	0.29					2.18		
Black locust [26]	650 °C for 3 h	Steam activation at 830 °C		1,175	0.55	0.49	83.43	1.52	0	15.05	1.85	2.79	0.75
		KOH activation at 830 °C for 1.5 h (Char: KOH =1:6)		2,064	0.98	0.87	74.36	1.15	0.00	24.49	3.75	5.86	1.21
Yellow mombin fruit stones [27]	500 °C for 3 h			252	0.14							5.80	
	700 °C for 3 h			358	0.17							7.00	
	400 °C for 4 h	KOH activation at 500 °C		1,384	0.63							8.60	
	400 °C for 4 h	KOH activation at 700 °C		2,290	1.19							10.50	
1 g Gelatin + 2 g Starch [28]	450 °C with heating rate of 10 °C/min	KOH activation at 700 °C for 10 min (porous carbon/KOH = ¼)		1,714	0.83		75.90	2.17	0.65	12.76	3.28		
1 g Gelatin + 1 g Starch [28]				1,636	0.51		71.40	3.75	3.00	21.12	3.84		

2 g Gelatin + 1 g Starch [28]				1,957	0.79		71.20	1.97	2.75	19.57	3.45		
1 g Gelatin [28]				1,294	0.63		74.48	2.42	0.39	16.60	3.30		
1 g Starch [28]				714	0.40		70.85	2.43		18.90	2.81		
Rice husk [29]	520 °C for 20 min	KOH activation at 400 °C for 30 min	KOH (1) activation at 640 °C for 1 h	774	0.41	0.30			0.75		3.53	4.88	1.51 (1.24)
			KOH (1) activation at 710 °C for 1 h	1,041	0.53	0.42			0.48		4.16	5.63	1.55 (1.21)
			KOH (1) activation at 780 °C for 1 h	1,199	0.60	0.48			0.36		3.87	6.02	1.28 (1.01)
			KOH (3) activation at 780 °C for 1 h	2,695	1.14	1.11			0.45		3.71	6.24	0.92 (0.69)
Peanut shell [30]	550 °C for 30 min	KOH activation at 680 °C for 1.5 h (KOH/ char =2:1)		1,713	0.73	0.73	88.00	1.10	0.98		4.41	7.25	

		KOH activation at 730 °C for 1.5 h (KOH/ char =2:1)		1,893	0.79	0.78	89.70	0.80	0.79		4.22	7.12	
		KOH activation at 780 °C for 1.5 h (KOH/ char =2:1)		1,871	0.80	0.79	90.50	0.60	0.60		3.92	6.79	
	400 °C for 1 h	KOH (2) activation at 600 °C for 2 h		1,473	0.60	0.57			3.81		4.18		(0.91)
	500 °C for 1 h	KOH (2) activation at 600 °C for 2 h		1,913	0.78	0.74			2.32		4.02		(0.67)
	600 °C for 1 h	KOH (2) activation at 600 °C for 2 h		1,698	0.70	0.62			2.56		3.52		(0.73)
	400 °C for 1 h	KOH (2) activation at 500 °C for 2 h		1,123	0.47	0.43			4.01		4.12		(1.04)
Poplar anthers [31]	400 °C for 1 h	KOH (2) activation at 700 °C for 2 h		1,976	0.86	0.77			3.11		3.93		(0.79)
	400 °C for 1 h	KOH (2) activation at 800 °C for 2 h		2,356	1.26	0.86			1.50		3.30		(0.53)
	400 °C for 1 h	KOH (1) activation at 600 °C for 2 h		837	0.38	0.32			4.84		3.61		(1.06)
	400 °C for 1 h	KOH (4) activation at 600 °C for 2 h		2,571	1.15	1.02			2.22		3.39		(0.57)
	500 °C for 1 h	KOH (4) activation at 800 °C for 2 h		3,322	2.31	0.89			1.26		2.04		(0.25)

Pine nut shell [32]	500 °C for 1.5 h	KOH (0.5) activation at 700 °C for 1.5 h		966	0.40						3.50		
		KOH (1) activation at 700 °C for 1.5 h		1,004	0.43						4.50		
		KOH (2) activation at 700 °C for 1.5 h		1,486	0.64						5.00		
		KOH (3) activation at 700 °C for 1.5 h		1,682	0.70						4.60		
		KOH (4) activation at 700 °C for 1.5 h		1,944	0.81						4.00		
		KOH (2) activation at 500 °C for 1.5 h		459	0.20						3.20		
		KOH (2) activation at 600 °C for 1.5 h		1,343	0.56						4.70		
		KOH (2) activation at 800 °C for 1.5 h		1,637	0.71						4.30		
		KOH (2) activation at 900 °C for 1.5 h		2,207	1.23						3.50		
Macadamia nut shells [33]	400 °C for 1 h	CO_2 activation at 900 °C for 15 min		469							3.07		
	400 °C for 1 h	CO_2 activation at 900 °C for 30 min		489							3.30		

	400 °C for 1 h	CO_2 activation at 900 °C for 60 min		606							3.40		
	500 °C for 1 h	CO_2 activation at 900 °C for 15 min		425							2.80		
	500 °C for 1 h	CO_2 activation at 900 °C for 30 min		514							3.25		
	500 °C for 1 h	CO_2 activation at 900 °C for 60 min		605							3.45		
	600 °C for 1 h	CO_2 activation at 900 °C for 15 min		441							2.99		
	600 °C for 1 h	CO_2 activation at 900 °C for 30 min		512							3.37		
	600 °C for 1 h	CO_2 activation at 900 °C for 60 min		573							3.48		
	700 °C for 1 h	CO_2 activation at 900 °C for 15 min		434							3.01		
	700 °C for 1 h	CO_2 activation at 900 °C for 30 min		524							3.42		
	700 °C for 1 h	CO_2 activation at 900 °C for 60 min		633							3.73		
Pineapple waste [34]	Hydrothermal carbonization at 210 °C for 10 h using $Li_2C_2O_4$	500 °C for 2 h		124			84.82	1.56	1.30		1.16	1.39	

	Hydrothermal carbonization at 210 °C for 10 h using $Na_2C_2O_4$			224.1			86.06	1.55	1.69		1.18	1.37	
	Hydrothermal carbonization at 210 °C for 10 h using $K_2C_2O_4$			422.8			80.01	1.16	1.52		2.22	2.71	
	Hydrothermal carbonization at 210 °C for 10 h using $Li_2C_2O_4$	600 °C for 2 h		302.7			81.12	0.75	1.30		1.59	2.09	
	Hydrothermal carbonization at 210 °C for 10 h using $Na_2C_2O_4$			328.2			84.98	0.20	1.59		1.33	1.65	
	Hydrothermal carbonization at 210 °C for 10 h using $K_2C_2O_4$			644.9			73.52	1.09	1.49		3.16	3.82	
	Hydrothermal carbonization at 210 °C for 10 h using $Li_2C_2O_4$	700 °C for 2 h		186			85.04	0.48	1.12		1.35	1.90	

	Hydrothermal carbonization at 210 °C for 10 h using $Na_2C_2O_4$			397.3			83.29	0.17	1.58		1.59	2.20	
	Hydrothermal carbonization at 210 °C for 10 h using $K_2C_2O_4$			1,076.3			86.31	0.14	0.33		4.25	5.32	

[a] S_{BET} stands for the specific surface area obtained by BET method; [b] V_{toal} stands for the total pore volume; [c] V_{micro} stands for the micropore volume.

[*] Calculated by difference.

[§] obtained at 30 °C; [ψ] obtained at 0 °C; ( ) obtained at 0.10 bar.

Table S2. *BWDPCs with heteroatom-doping treatment.*

Carbon Precursors	Upcycling into Porous Carbons			Textural Properties			Ultimate analysis (%)				CO_2 uptake (mmol/g)		
	Carbonization	Activation or Surface Modification	Activation or Surface Modification	S_{BET} [a] (m^2/g)	V_{toal} [b] (cm^3/g)	V_{micro} [c] (cm^3/g)	C	H	N	O*	25 °C and 1 bar	0 °C and 1 bar	25 °C and 0.15 bar
Agar [35]	500 °C for 2 h	$Zn(NO_3)_2$ (4) activation at 700 °C for 2 h		671	0.43				10.55		2.30		
		$Zn(NO_3)_2$ (2) activation at 800 °C for 2 h		886	0.57				10.02		2.60		
		$Zn(NO_3)_2$ (4) activation at 800 °C for 2 h		1,033	0.69				9.71		2.40		
		$Zn(NO_3)_2$ (6) activation at 800 °C for 2 h		858	0.57				7.29		2.50		
		$Zn(NO_3)_2$ (4) activation at 900 °C for 2 h		1,142	0.85				6.65		2.50		
		$Zn(NO_3)_2$ (4) activation at 950 °C for 2 h		1,316	1.14				5.68		2.50		

Agar [36]		Urea (0.25) modification at 350 °C for 2 h	KOH activation at 600 °C for 1 h	1,005	0.49	0.40			5.11		3.70	6.00		
		Urea (0.5) modification at 350 °C for 2 h	KOH activation at 550 °C for 1 h	910	0.44	0.36			7.33		3.60	5.90		
		Urea (0.5) modification at 350 °C for 2 h	KOH activation at 600 °C for 1 h	1,239	0.61	0.48			6.08		3.70	6.50		
		Urea (0.5) modification at 350 °C for 2 h	KOH activation at 650 °C for 1 h	1,500	0.74	0.53			5.56		3.10	5.90		
		Urea (0.25) modification at 350 °C for 2 h	KOH activation at 700 °C for 1 h	1,830	0.91	0.42			5.07		2.50	4.60		
		Urea (0.75) modification at 350 °C for 2 h	KOH activation at 600 °C for 1 h	1,448	0.71	0.55			7.23		3.20	6.10		

		Urea (1.0) modification at 350 °C for 2 h	KOH activation at 600 °C for 1 h	1,423	0.71	0.53			8.58		3.20	5.80	
Hazelnut shell [37]	500 °C for 1 h	$NaNH_2$ (1) at 500 °C for 1 h		502	0.22		85.21	5.87	2.74		2.24		
		$NaNH_2$ (2) at 500 °C for 1 h		1,991	0.88		87.21	5.03	2.94		3.72		
		$NaNH_2$ (3) at 500 °C for 1 h		1,833	0.80		86.24	5.31	3.21		3.39		
		$NaNH_2$ (1) at 550 °C for 1 h		1,099	0.45		86.32	5.99	2.53		4.32		
		$NaNH_2$ (2) at 550 °C for 1 h		1,821	0.79		86.74	5.87	2.75		3.50		
		$NaNH_2$ (3) at 550 °C for 1 h		2,185	0.99		87.02	6.01	2.97		3.48		
		$NaNH_2$ (1) at 600 °C for 1 h		1,343	0.55		87.65	5.24	1.98		3.94		
		$NaNH_2$ (2) at 600 °C for 1 h		2,318	1.03		88.34	5.87	2.14		3.52		
		$NaNH_2$ (3) at 600 °C for 1 h		2,321	1.11		88.21	5.21	2.30		3.38		

Walnut shell powders [38]	H_3PO_4 activation at 150 °C for 12 h	Urea modification at 350 °C for 2 h	KOH (1.5) activation at 650 °C for 1 h	759	0.44	0.33	51.21	1.96	4.45		2.32	3.30	
			KOH (2.5) activation at 650 °C for 1 h	1,606	0.97	0.78	71.19	2.88	4.02		1.92	2.90	
			KOH (3.5) activation at 650 °C for 1 h	1,741	0.86	0.80	64.43	3.21	2.20		2.74	4.73	
			KOH (1.5) activation at 750 °C for 1 h	1,636	0.74	0.68	54.00	3.75	2.69		2.86	5.00	
			KOH (2.5) activation at 750 °C for 1 h	2,251	1.21	1.03	70.44	1.62	0.94		2.54	4.20	
			KOH (3.5) activation at 750 °C for 1 h	3,079	1.84	1.18	80.49	1.20	2.08		2.53	3.35	

			KOH (1.5) activation at 850 °C for 1 h	2,354	1.26	0.97	75.38	1.30	0.86		3.04	5.13	
			KOH (2.5) activation at 850 °C for 1 h	2,556	1.90	0.96	81.84	1.75	0.76		2.27	3.35	
			KOH (3.5) activation at 850 °C for 1 h	1,000	0.68	0.53	51.67	1.75	1.57		2.37	2.57	
Walnut shell [39]	150 °C for 12 h	Urea modification at 350 °C for 2 h	KOH activation at 750 °C for 1 h	1,636	0.74	0.68	54.00	3.75	2.69	39.56	2.86		0.67
			KOH activation at 850 °C for 1 h	2,354	1.26	0.97	75.38	1.30	0.86	22.46	3.08		0.64
			K_2CO_3 activation at 750 °C for 1 h	1,144	0.64	0.48	68.18	1.57	4.80	25.45	2.10		0.36

			K_2CO_3 activation at 850 °C for 1 h	1,813	1.05	0.70	80.95	0.79	1.00	17.26	2.14		0.38
			$ZnCl_2$ activation at 750 °C for 1 h	273	0.19	0.13	46.52	1.55	9.32	42.61	1.78		0.69
			$ZnCl_2$ activation at 850 °C for 1 h	481	0.27	0.24	52.01	1.92	8.75	37.32	1.83		0.67
Walnut shell [40]	500 °C for 1 h	$NaNH_2$ (1.5) modification at 400 °C for 1 h		419	0.25	0.19	54.24	3.37	3.79		1.93	2.60	
		$NaNH_2$ (1.5) modification at 450 °C for 1 h		589	0.34	0.27	63.53	4.38	7.24		2.53	4.17	
		$NaNH_2$ (1.5) modification at 500 °C for 1 h		802	0.47	0.37	57.60	3.45	1.52		1.96	3.88	
		$NaNH_2$ (2.5) modification at 400 °C for 1 h		516	0.28	0.20	52.55	3.35	3.52		1.70	2.67	

		$NaNH_2$ (2.5) modification at 450 °C for 1 h		1,687	0.94	0.77	72.63	3.18	1.89		3.06	5.22	
		$NaNH_2$ (2.5) modification at 500 °C for 1 h		1,721	0.92	0.75	61.53	1.45	2.54		2.15	3.17	
Tea seed shell [41]	700 °C for 2 h	KOH activation at 700 °C for 2 h	Melamine (1) modification at 700 °C for 2 h	1,065	0.47	0.39	59.43	1.24	2.43		2.69		
			Melamine (2) modification at 700 °C for 2 h	1,188	0.52	0.44	66.21	0.94	3.41		2.75		
			Melamine (3) modification at 700 °C for 2 h	1,055	0.46	0.39	61.47	1.16	3.45		2.44		
			Melamine (4) modification at 700 °C for 2 h	706	0.33	0.25	48.26	1.77	3.39		1.95		

Water chestnut shell [42]	500 °C for 2 h	$NaNH_2$ (1) activation at 400 °C for 2 h		669	0.31		71.42	3.06	3.05		3.29		
		$NaNH_2$ (2) activation at 400 °C for 2 h		1,450	0.61		73.24	2.99	3.26		3.63		
		$NaNH_2$ (3) activation at 400 °C for 2 h		1,310	0.65		74.25	3.01	3.58		3.18		
		$NaNH_2$ (1) activation at 450 °C for 2 h		1,036	0.44		76.21	3.01	2.73		4.06		
		$NaNH_2$ (2) activation at 450 °C for 2 h		2,412	1.14		75.20	2.75	3.14		4.04		
		$NaNH_2$ (3) activation at 450 °C for 2 h		2,596	1.42		73.58	2.80	3.35		3.59		
		$NaNH_2$ (1) activation at 500 °C for 2 h		1,416	0.58		77.43	2.42	2.42		4.50		
		$NaNH_2$ (2) activation at 500 °C for 2 h		2,615	1.38		76.52	2.53	2.68		3.60		

		$NaNH_2$ (3) activation at 500 °C for 2 h		2,446	1.59		76.03	2.86	3.12		3.39		
Palm kernel shell [43]	500 °C for 1 h	Urea (3) modification at 600 °C for 1 h		852	0.38	0.31	85.90		3.03	10.87	4.39		
		Urea (3) modification at 700 °C for 1 h		1,185	0.52	0.43	90.97		3.35	5.54	4.80		
		Urea (3) modification at 800 °C for 1 h		694	0.37	0.25	88.31		1.95	9.53	3.39		
		Urea (1) modification at 700 °C for 1 h		699	0.49	0.16	92.63		1.73	5.45	2.56		
		Urea (5) modification at 700 °C for 1 h		586	0.31	0.19	88.52		2.94	8.24	2.84		
Water chestnut [44]		Melamine modification at 500 °C for 2 h	KOH activation at 600 °C for 1 h	2,998	1.78	1.22			7.50		3.60		

			KOH activation at 650 °C for 1 h	3,277	1.94	1.37			5.50		4.10		
			KOH activation at 700 °C for 1 h	3,401	2.50	1.87			4.89		4.70		
			KOH activation at 800 °C for 1 h	3,138	2.43	1.33			2.73		3.20		
Coconut shell [45]	500 °C for 2 h	Urea modification at 350 °C for 2 h	K_2CO_3 (2) activation at 600 °C for 1 h	947	0.35		86.59	0.94	2.76		3.45		
			K_2CO_3 (3) activation at 600 °C for 1 h	1,082	0.39		87.48	0.88	2.74		3.71		
			K_2CO_3 (4) activation at 600 °C for 1 h	1,324	0.51		91.35	0.82	1.52		3.49		

			K_2CO_3 (2) activation at 700 °C for 1 h	1,199	0.47		91.08	0.52	1.42		3.07		
			K_2CO_3 (3) activation at 700 °C for 1 h	1,354	0.58		88.71	0.55	1.34		3.03		
			K_2CO_3 (2) activation at 800 °C for 1 h	1,329	0.56		91.35	0.56	1.13		2.86		
			K_2CO_3 (3) activation at 800 °C for 1 h	1,430	0.65		93.24	0.65	0.86		2.78		
Coconut shell [46]	500 °C for 2 h	Urea modification at 350 °C for 2 h	KOH (2) activation at 600 °C for 1 h	1,023	0.38		84.20	1.52	1.35		4.10		
			KOH (3) activation at 600 °C for 1 h	1,383	0.56		83.30	1.32	1.08		4.00		

			KOH (4) activation at 600 °C for 1 h	1,604	0.65		84.20	1.53	0.81		4.30		
			KOH (2) activation at 650 °C for 1 h	1,178	0.49		82.00	1.34	1.23		4.10		
			KOH (3) activation at 650 °C for 1 h	1,535	0.60		81.30	1.22	0.91		4.80		
			KOH (4) activation at 650 °C for 1 h	1,687	0.67		83.00	1.29	0.70		4.30		
			KOH (2) activation at 700 °C for 1 h	1,550	0.62		84.20	1.03	0.86		4.10		
			KOH (3) activation at 700 °C for 1 h	1,596	0.64		86.30	0.92	0.73		4.70		

			KOH (4) activation at 700 °C for 1 h	1,937	0.78		86.50	0.84	0.61		4.44		
		KOH (3) activation at 650 °C for 1 h	Urea modification at 350 °C for 2 h	1,012	0.44		75.50	0.95	8.01		3.00		
Coconut shell [47]	500 °C for 2 h	Ammonia modification at 350 °C for 5 h	KOH (1) activation at 600 °C for 2 h	879	0.38		64.20	4.02	6.16		3.68		
			KOH (2) activation at 600 °C for 2 h	1,135	0.62		70.50	3.38	4.83		4.04		
			KOH (3) activation at 600 °C for 2 h	1,850	0.87		69.80	3.00	4.31		4.16		
			KOH (4) activation at 600 °C for 2 h	1,562	0.75		69.00	2.69	3.84		3.79		

			KOH (1) activation at 650 °C for 2 h	1,483	0.66		70.00	2.67	4.56		4.26		
			KOH (2) activation at 650 °C for 2 h	1,487	0.79		71.20	2.45	3.59		4.22		
			KOH (3) activation at 650 °C for 2 h	2,322	1.06		74.10	2.80	3.19		4.10		
			KOH (4) activation at 650 °C for 2 h	2,521	1.34		75.80	2.48	2.40		3.72		
			KOH (1) activation at 700 °C for 2 h	2,349	0.99		77.30	2.03	2.22		4.22		
			KOH (2) activation at 700 °C for 2 h	1,967	0.94		79.20	2.22	1.81		4.09		

			KOH (3) activation at 700 °C for 2 h	2,690	1.19		78.30	2.46	1.70		3.96		
			KOH (4) activation at 700 °C for 2 h	2,599	1.33		80.70	2.11	1.21		3.44		
Argan hard shell [48]	700 °C for 1 h	KOH activation at 850 °C for 1 h (PM)		2,251	1.04	0.93	85.08		9.49	5.43	5.51		
		KOH activation at 850 °C for 1 h (IM)		1,890	0.87	0.80	82.68		13.90	3.42	5.63		
		NaOH activation at 850 °C for 1 h (PM)		1,463	0.74	0.58	67.74		9.07	23.19	3.64		
		NaOH activation at 850 °C for 1 h (IM)		1,827	0.96	0.73	82.14		12.61	5.25	3.73		
Longan shells [49]	500 °C for 2 h under N_2/carbamide atmosphere	KOH activation at 600 °C for 2 h		1,529	0.98							3.20	
		KOH activation at 700 °C for 2 h		2,209	1.30							4.30	

		KOH activation at 800 °C for 2 h		3,260	2.60							5.60	
		KOH activation at 900 °C for 2 h		2,734	2.30							4.80	
Black gram [50]	300 °C for 4 h	KOH (1) activation at 650 °C for 1 h		956	0.48	0.31	76.95	2.39	4.82		3.34	4.61	
		KOH (1) activation at 700 °C for 1 h		1,258	0.61	0.40	83.63	2.90	4.21		3.46	5.30	
		KOH (1) activation at 750 °C for 1 h		1,697	0.82	0.37	84.08	2.06	3.86		3.46	5.25	
		KOH (1) activation at 800 °C for 1 h		1,987	1.02	0.26	89.43	1.41	1.78		2.76	5.10	
		KOH (2) activation at 650 °C for 1 h		990	0.42	0.31	79.99	2.90	4.76		3.25	4.65	
		KOH (2) activation at 700 °C for 1 h		1,428	0.65	0.29	78.36	2.58	4.38		3.06	4.97	

		KOH (2) activation at 750 °C for 1 h		1,675	0.96	0.06	75.76	2.51	3.67		2.28	3.90	
		KOH (2) activation at 800 °C for 1 h		2,086	1.08	0.16	91.38	1.06	2.52		2.59	4.69	
		KOH (3) activation at 650 °C for 1 h		1,216	0.53	0.35	78.46	2.21	5.34		3.16	4.82	
		KOH (3) activation at 700 °C for 1 h		1,446	0.63	0.37	81.60	2.41	4.15		3.21	5.15	
		KOH (3) activation at 750 °C for 1 h		1,952	1.11	0.04	71.34	3.40	3.15		2.14	3.73	
		KOH (3) activation at 800 °C for 1 h		2,305	1.23	0.13	79.17	2.13	1.81		2.34	4.79	
Oil residue [51]	500 °C for 1 h	$NaNH_2$ (1.5) activation at 450 °C for 2 h		660	0.42	0.33	57.89	2.71	4.31		2.04		
		$NaNH_2$ (2.5) activation at 450 °C for 2 h		846	0.94	0.40	56.50	2.52	4.59		2.11		

		$NaNH_2$ (1.5) activation at 500 °C for 2 h		1,176	0.72	0.57	60.87	3.01	5.83		2.19		
		$NaNH_2$ (2.5) activation at 500 °C for 2 h		2,113	1.24	0.94	61.07	1.98	6.90		3.51		
		$NaNH_2$ (1.5) activation at 550 °C for 2 h		1,508	0.94	0.68	62.98	2.10	6.02		3.42		
		$NaNH_2$ (2.5) activation at 550 °C for 2 h		2,148	1.32	0.94	64.49	1.70	5.57		2.98		
		CO_2 activation at 800 °C for 2 h		748	0.47	0.27	83.84	0.04	1.10	15.02	2.55		
Biomass glucose [52]	80 °C for 24 h with CTAB	CO_2 activation at 800 °C for 2 h	Urea modification at 350 °C for 2 h	697	0.46	0.25	75.15	0.05	6.50	18.30	2.92		
		Urea modification at 350 °C for 2 h	500 °C for 2 h (N_2)	581	0.35	0.21	67.78	1.14	11.48	19.50	3.03		
Poplar catkins [53]	400 °C for 3 h	$ZnCl_2$ (4) activation at 700 °C for 2 h		1,361.9	0.58	0.46	87.23	1.62	1.89	9.26	3.55		

		$ZnCl_2$ (2) activation at 800 °C for 2 h		1,005.4	0.41	0.34	87.42	1.32	2.37	8.89	3.75		
		$ZnCl_2$ (4) activation at 800 °C for 2 h		1,455.1	0.68	0.47	88.57	0.89	2.89	7.65	4.05		
		$ZnCl_2$ (6) activation at 800 °C for 2 h		1,248.7	0.50	0.41	89.74	0.78	2.16	7.32	2.62		
		$ZnCl_2$ (4) activation at 900 °C for 2 h		1,272.4	0.55	0.43	89.23	0.82	2.09	7.86	3.35		
d-glucose [54]	180 °C for 12 h	KOH (1) activation at 600 °C for 1 h		821	0.42		65.54	2.14	12.17		3.99	5.33	
		KOH (2) activation at 600 °C for 1 h		1,267	0.54		64.89	2.15	11.93		4.24	6.23	
		KOH (3) activation at 600 °C for 1 h		1,398	0.60		63.54	2.16	11.67		4.02	6.11	
		KOH (4) activation at 600 °C for 1 h		1,412	0.63		62.21	2.12	11.23		3.93	5.90	

		KOH (1) activation at 650 °C for 1 h		1,734	0.78		75.01	1.41	9.24		4.26	6.70	
		KOH (2) activation at 650 °C for 1 h		1,960	0.90		74.32	1.35	8.56		4.23	6.14	
		KOH (3) activation at 650 °C for 1 h		2,167	0.96		72.68	1.37	7.23		4.21	6.28	
		KOH (4) activation at 650 °C for 1 h		2,016	0.94		75.35	1.17	6.85		4.07	6.11	
		KOH (1) activation at 700 °C for 1 h		2,394	1.13		81.51	0.89	6.94		3.92	6.46	
		KOH (2) activation at 700 °C for 1 h		2,659	1.32		79.12	0.75	6.72		3.71	5.73	
		KOH (3) activation at 700 °C for 1 h		2,655	1.40		77.05	0.85	6.43		3.51	5.36	
		KOH (4) activation at 700 °C for 1 h		2,470	1.30		76.92	0.96	6.20		3.42	5.24	

d-glucose [55]		Melamine modification at 500 °C for 1 h	KOH (2) activation at 700 °C for 2 h	1,210	0.69		74.30		9.80		4.18		
			KOH (2) activation at 800 °C for 2 h	1,780	1.35		82.50		6.94		4.66		
			KOH (3) activation at 700 °C for 2 h	2,136	1.43		80.80		6.84		3.89		
			KOH (3) activation at 800 °C for 2 h	3,247	3.09		86.90		2.07		4.95		
d-glucose [56]	180 °C for 12 h	Urea modification at 350 °C for 1 h	K_2CO_3 (2) activation at 600 °C for 1 h	933	0.45		66.51	2.33	12.27		3.43	4.80	
			K_2CO_3 (3) activation at 600 °C for 1 h	1,005	0.46		65.31	2.38	12.21		3.46	4.84	

			K_2CO_3 (4) activation at 600 °C for 1 h	1,170	0.53		63.67	2.42	11.81		3.74	5.32	
			K_2CO_3 (2) activation at 650 °C for 1 h	1,754	0.83		69.83	2.14	10.51		3.69	5.45	
			K_2CO_3 (3) activation at 650 °C for 1 h	1,699	0.89		70.32	1.98	9.54		3.65	5.87	
			K_2CO_3 (4) activation at 650 °C for 1 h	1,824	0.92		71.66	1.97	7.74		3.92	6.23	
			K_2CO_3 (2) activation at 700 °C for 1 h	2,572	1.43		77.70	1.56	6.57		3.75	6.23	
			K_2CO_3 (3) activation at 700 °C for 1 h	2,510	1.54		80.32	1.73	5.03		3.56	6.16	

			K_2CO_3 (4) activation at 700 °C for 1 h	2,827	1.55		84.24	1.65	4.69		3.61	6.05	
d-glucose [55]	500 °C for 1 h	KOH (2) activation at 700 °C for 2 h		1,210	0.69		74.30		9.80		4.18	6.11	
		KOH (2) activation at 800 °C for 2 h		1,780	1.35		82.50		6.94		4.66	7.77	
		KOH (3) activation at 700 °C for 2 h		2,136	1.43		80.80		6.84		3.89	7.43	
		KOH (3) activation at 800 °C for 2 h		3,247	3.09		86.90		2.07		4.95	8.07	
Glucose [12]	Hydrothermal carbonization at 180 °C for 10 h with Ethylenediamine	KOH activation at 500 °C for 1 h		1,082	0.58	0.44			9.44	12.65	3.78	5.36	1.29
		KOH activation at 600 °C for 1 h		1,793	0.87	0.73			8.02	10.86	5.01	7.60	1.38
		KOH activation at 700 °C for 1 h		2,328	1.11	0.94			5.05	10.04	4.32	7.18	0.93
		KOH activation at 800 °C for 1 h		2,958	1.61	1.16			2.73	4.47	3.36	6.24	0.65

Lignin [57]	200 °C for 12 h	KOH activation at 700 °C for 2 h	Urea (1) modification at 800 °C for 1 h	3,020	1.89		80.03		0.62	19.34	2.20		
		KOH activation at 700 °C for 2 h	Urea (2) modification at 800 °C for 1 h	3,064	1.56		87.10		0.64	12.26	2.50		
		KOH activation at 700 °C for 2 h	Urea (4) modification at 800 °C for 1 h	3,021	1.58		89.55		1.10	9.35	2.60		
		KOH activation at 700 °C for 2 h	Urea (8) modification at 800 °C for 1 h	2,473	1.26		87.81		1.17	11.02	2.70		
Lignin [58]	300 °C for 0.5 h	KOH/adenine activation at 700 °C for 1 h		1,788	0.91	0.49	40.40		5.60	54.00	4.80	8.20	
		KOH/adenine activation at 850 °C for 1 h		2,957	1.79	0.56	59.50		2.50	38.00	4.40	7.60	

		KOH/adenine activation at 1000 °C for 1 h		1,075	0.75	0.21	64.00		2.20	33.80	4.00	6.50	
De-alkaline lignin [59]		KOH (1) activation at 800 °C	NH_3 modification at 800 °C	2,922	1.36	1.22					5.12		
		KOH (2) activation at 800 °C		2,779	1.39	1.10					5.48		
		KOH (3) activation at 800 °C		1,631	0.83	0.60					4.23		
Sugarcane bagasse [60]		Urea modification at 600 °C for 0.5 h		32	0.02		83.16	1.74	3.81		1.94		
		Urea (5) modification at 600 °C for 0.5 h	KOH (2) activation at 600 °C for 1 h	851	0.44		87.00	0.97	0.83		4.52		
		Urea (10) modification at 600 °C for 0.5 h		927	0.48		83.26	1.17	1.76		4.60		
		Urea (15) modification at 600 °C for 0.5 h		1,113	0.57		83.59	1.18	1.98		4.80		

		Urea (20) modification at 600 °C for 0.5 h		1,024	0.53		83.02	1.16	1.98		4.76		
		Urea (25) modification at 600 °C for 0.5 h		945	0.49		84.19	1.12	1.99		4.71		
Lotus stalks [61]	500 °C for 2 h	$NaNH_2$ (1) activation at 400 °C for 1 h		848	0.38		67.03	2.34	3.77		3.39		
		$NaNH_2$ (2) activation at 400 °C for 1 h		1,164	0.54		68.32	2.55	4.01		3.67		
		$NaNH_2$ (3) activation at 400 °C for 1 h		1,087	0.52		67.65	2.25	4.50		3.22		
		$NaNH_2$ (1) activation at 450 °C for 1 h		1,105	0.49		70.25	2.12	3.21		3.69		
		$NaNH_2$ (2) activation at 450 °C for 1 h		2,053	0.97		71.37	2.04	3.64		3.47		
		$NaNH_2$ (3) activation at 450 °C for 1 h		1,921	1.04		70.98	2.06	4.03		3.12		

		$NaNH_2$ (1) activation at 500 °C for 1 h		1,113	0.48		73.56	2.09	2.61		3.88		
		$NaNH_2$ (2) activation at 500 °C for 1 h		2,264	1.34		74.32	1.97	3.08		3.51		
		$NaNH_2$ (3) activation at 500 °C for 1 h		1,824	1.03		74.98	1.88	3.45		3.45		
Commercial phenolic resins [62]	500 °C for 2 h	$NaNH_2$ (1) activation at 400 °C for 1 h		735	0.31		77.70	2.58	2.72		3.32		
		$NaNH_2$ (2) activation at 400 °C for 1 h		936	0.39		78.36	2.29	4.56		4.12		
		$NaNH_2$ (3) activation at 400 °C for 1 h		1,115	0.46		79.36	2.43	5.36		4.14		
		$NaNH_2$ (4) activation at 400 °C for 1 h		1,003	0.41		79.11	2.16	6.05		3.83		
		$NaNH_2$ (1) activation at 450 °C for 1 h		787	0.33		80.60	2.42	1.56		3.86		

		$NaNH_2$ (2) activation at 450 °C for 1 h		1,088	0.45		79.32	2.36	3.90		4.06		
		$NaNH_2$ (3) activation at 450 °C for 1 h		1,432	0.59		78.62	1.76	4.25		4.64		
		$NaNH_2$ (4) activation at 450 °C for 1 h		1,569	0.64		77.65	2.24	5.94		4.40		
		$NaNH_2$ (1) activation at 500 °C for 1 h		932	0.39		85.36	1.95	1.39		4.03		
		$NaNH_2$ (2) activation at 500 °C for 1 h		1,288	0.54		83.69	1.70	3.85		4.61		
		$NaNH_2$ (3) activation at 500 °C for 1 h		1,924	0.79		81.34	1.64	4.09		4.57		
		$NaNH_2$ (4) activation at 500 °C for 1 h		2,155	0.94		76.96	1.29	5.74		4.38		
Biomass canes [63]		Urea modification at 600 °C for 2 h		18	0.02		80.03		13.53	5.76	1.50		

		Urea/KOH modification at 600 °C for 2 h		982	0.62		79.26		8.12	11.89	2.20		
		Urea/$ZnCl_2$ modification at 600 °C for 2 h		582	0.29		74.73		15.88	7.28	2.10		
Pigskin [64]		$Ca(NO_3)_2/K_2CO_3$ modification at 600 °C for 2 h		1,165	1.03		64.70	1.50	10.40	23.25	4.40	5.30	
		$Ca(NO_3)_2/K_2CO_3$ modification at 700 °C for 2 h		2,693	1.68		84.80	0.50	6.20	8.21	3.10	4.70	
		$Ca(NO_3)_2/K_2CO_3$ modification at 800 °C for 2 h		2,731	1.89		86.80	1.80	2.60	7.90	2.50	4.10	
		$Ca(NO_3)_2/K_2CO_3$ modification at 900 °C for 2 h		2,799	1.91		91.90	1.20	1.60	4.45	2.20	4.00	
Chitosan [65]	550 °C for 0.5 h	KOH activation at 400 °C for 0.5 h	600 °C for 1.5 h with 100 mL/min	667	0.29	0.28	63.30	2.40	6.50		3.74		1.46
			600 °C for 1.5 h with 450 mL/min	716	0.32	0.31	61.50	2.50	6.60		4.04		1.57

			600 °C for 1.5 h with 800 mL/min	718	0.33	0.31	59.10	2.30	6.80		4.17		1.86
			600 °C for 1.5 h with 1040 mL/min	907	0.40	0.39	57.90	2.60	6.70		4.26		1.77
Rotten strawberries [66]	180 °C for 12 h	KOH (2) activation at 600 °C for 1 h		935	0.42		72.21	2.55	3.68		3.63		
		KOH (4) activation at 600 °C for 1 h		1,441	0.60		68.99	2.21	5.16		4.04		
		KOH (2) activation at 650 °C for 1 h		1,117	0.52		78.02	2.44	5.38		4.49		
		KOH (4) activation at 650 °C for 1 h		1,482	0.64		70.16	3.06	5.06		3.87		
		KOH (2) activation at 700 °C for 1 h		1,408	0.67		76.23	2.39	3.81		3.73		
		KOH (4) activation at 700 °C for 1 h		1,577	0.68		79.18	2.11	2.60		3.99		

Soya chunks [67]	180 °C for 12 h	NaOH activation at 600 °C for 1 h	900 °C for 2 h	607					4.30		2.70		
			1000 °C for 2 h	1,072					5.30		3.20		
Arundo donax [68]		$ZnCl_2$ activation at 500 °C for 1 h		1,863	1.00				5.40		2.10		
		$ZnCl_2$ activation at 600 °C for 1 h		1,340	0.68				4.05		1.70		
		$ZnCl_2$ activation at 700 °C for 1 h		1,420	0.76				3.50		2.00		
Waste wool [69]	300 °C for 2 h	KOH (1) activation at 600 °C for 1 h		447	0.22	0.18	71.90	1.37	11.25	15.48	1.48		
		KOH (3) activation at 600 °C for 1 h		1,010	0.57	0.37	70.73	1.64	4.57	23.06	2.33		
		KOH (5) activation at 600 °C for 1 h		1,352	0.78	0.54	69.65	1.42	4.14	24.79	2.78		
Fallen leaves [70]	600 °C for 2 h	KOH (2) activation at 600 °C for 1 h		1,210	0.48	0.39	84.80		1.70		3.39		1.20

		KOH (1) activation at 700 °C for 1 h		1,360	0.51	0.40	81.30		1.00		4.09		1.55
		KOH (2) activation at 700 °C for 1 h		1,600	0.65	0.54	84.40		1.30		4.41		1.41
		KOH (2) activation at 700 °C for 1 h (H)		1,630	0.66	0.56	85.50		2.50		4.20		1.14
		KOH (3) activation at 700 °C for 1 h		2,230	1.03	0.89	86.50		0.40		3.93		0.98
		KOH (2) activation at 800 °C for 1 h		1,950	0.88	0.72	84.80		0.40		4.23		1.14
Coffee grounds (Nespresso) [71]	400 °C for 1 h	APTES modification at 80 °C for 24 h		0.8	0.01	<0.01			0.41	0.8	0.41 §		
			KOH activation at 600 °C for 1 h	1,684	0.94	0.45			2.04	1684	2.04 §		
		Aniline		22	0.12	<0.01			0.46	22	0.46 §		

		modification at 0 °C for 6 h	KOH activation at 600 °C for 1 h	992	0.61	0.37			2.22	992	2.22 §		
		Melamine modification at 160 °C for 24 h		402	0.22	0.09			0.85	402	0.85 §		
			KOH activation at 600 °C for 1 h	990	0.55	0.45			2.67	990	2.67 §		
Stem bark [72]	170 °C for 10 h	KOH activation at 700 °C for 1 h		1,393	0.63	0.49	87.48		1.61	10.91	3.92		
		KOH activation at 800 °C for 1 h		1,759	0.92	0.60	89.48		1.43	9.09	4.45		
		KOH activation at 900 °C for 1 h		1,229	0.89	0.15	92.59		0.99	6.42	3.76		
Black locust [26]	650 °C for 3 h	KOH activation at 830 °C for 1.5 h		2,511	1.35	1.16	76.38	1.48	7.21		5.05	7.19	1.59
Banana peel [73]	800 °C for 1 h	CO_2 activation at 800 °C for 1 h		1,426.1	0.83	0.56	43.50	2.20	4.20		2.70		
Coca cola [74]		ammonia/CTAB modification at 400 °C for 4 h	$ZnCl_2$ (1) activation at 800 °C for 2 h	1,082	0.43		69.60		3.30	13.80	3.20		

			$ZnCl_2$ (2) activation at 800 °C for 2 h	1,994	0.87		73.10		4.20	10.30	3.08		
			KOH (1) activation at 800 °C for 2 h	1,405	0.80		74.00		3.50	12.50	5.22		
Human hair [75]		KOH activation at 550 °C for 1 h		1,230	0.90							5.14	
		KOH activation at 650 °C for 1 h		2,380	1.64							5.45	
		KOH activation at 750 °C for 1 h		2,700	1.33							4.27	
Olive stones [76]		700 °C for 5.5 h under 3 vol% O_2/N_2 atmosphere		514	0.21				0.40	7.40			0.88
		CO_2 activation at 800 °C for 6 h		1,248	0.44				0.70	11.30			0.99
Coffee [76]		CO_2 activation at 700 °C for 8 h		534	0.25				4.10	12.20			1.11
Almond shells [76]		CO_2 activation at 800 °C for 4 h		847	0.34				1.30	16.80			0.98

Grape seed [76]		CO_2 activation at 800 °C for 0.5 h		535	0.23				1.80	12.90			0.91
	200 °C for 12 h			362	0.27				2.20	7.80			0.91

[a] S_{BET} stands for the specific surface area obtained by BET method; [b] V_{toal} stands for the total pore volume; [c] V_{micro} stands for the micropore volume.

[*] Calculated by difference.

[§] obtained at 35 °C.

S1. Data Pre-processing

After data collection, as described in the section on Data Collection and Formatting in the main manuscript, it was observed that the CO_2 adsorbed on BWDPCs was reported either in mmol/g or mg/g units. To ensure unit consistency, we transformed all CO_2 adsorption data units into mmol/g. Similarly, it was observed that the pressures at which the adsorption experiments were performed were reported in different units including bar, atm, mmHg, and kPa. For this reason, all the pressure-related data were converted into bars to ensure unit consistency for further modeling applications.

S2. Missing Data Imputation

As described in the Data Pre-processing section of the main manuscript, during the data collection process, most publications have reported data on the surface area (SA), and they were complemented either with the total pore volume (TPV) or micropore volume (MPV); in several instances, all three variables were used. As a result, each unique row had missing data during the data collection process. Several rows of data had either SA or TPV, whereas MPV was missing, and in other cases, the data on SA and MPV were available, but TPV was missing. More specifically, of the 527 data points used in the study, 485 unique values were available for TPV (e.g., 7.8% missing data) and 296 data points for MPV (e.g., 44 % missing data). Table S3 provides descriptive statistics of the textural properties prior to data imputation.

Table S3. *Descriptive statistics of the textural properties prior to data imputation.*

Statistics	**SA (m^2/g)**	**TPV (cm^3/g)**	**MPV (cm^3/g)**
Datapoints	527	485	296
Mean	1,436	0.795	0.525
Std. deviation	764	0.455	0.276

Min	0.15	0.010	0.040
25% percentile	849	0.470	0.310
50% percentile	1,393	0.690	0.480
75% percentile	1,952	1.030	0.700
Max	3,337	3.090	1.290
% Missing data	N/A	7.800	44.000

Pearson's correlation coefficient (PCC) was performed to determine the extent of correlation among the three textural properties. The PCC revealed a strong and positive correlation among the three textural properties (Figure S1), and the PCC values between SA and TPV, SA and MPV, and TPV and MPV were 0.91, 0.78, and 0.69, respectively.

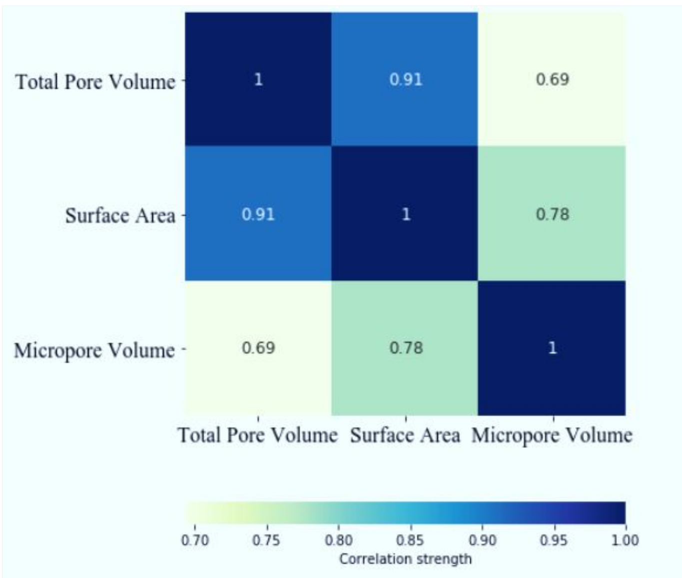

Figure S1. *PCC plot of the textural properties.*

Based on the significant correlation among the textural properties, the missing values of TPV and MPV were imputed by mapping them as a function of SA using two ML algorithms (linear regression and random forest).

***Table S4**. Comparative evaluation of linear regression and random forest model to map TPV and MPV as a function of SA.*

	Training R^2	Test R^2
Linear Regression	0.836	0.811
Random Forest	0.858	0.852

For each textural property, that is, TPV and MPV, the respective existing data points were split into an 80:20 ratio for training and testing. The corresponding SA value was used as the input feature. Linear regression and random forest models [77] were fitted to the training data using default hyperparameters. The mapping function devised on the training set for both models was then used to predict the values of TPV and MPV on the test set, in which the random forest model performed better than linear regression in terms of training and test R^2. Table S4 presents the evaluation metrics for the training and test sets for both models. Given the excellent performance of the random forest model in mapping TPV and MPV as a function of SA, the random forest model was eventually used to impute 42 data points for the TPV and 231 data points for MPV to attain a uniform master dataset, where all the individual features used in the study had 527 unique data points each.

REFERENCES

1. Dissanayake, P. D.; Choi, S. W.; Igalavithana, A. D.; Yang, X.; Tsang, D. C. W.; Wang, C.-H.; Kua, H. W.; Lee, K. B.; Ok, Y. S., Sustainable gasification biochar as a high efficiency adsorbent for CO_2 capture: A facile method to designer biochar fabrication. *Renewable and Sustainable Energy Reviews* **2020**, *124*, 109785.
2. Igalavithana, A. D.; Choi, S. W.; Dissanayake, P. D.; Shang, J.; Wang, C. H.; Yang, X.; Kim, S.; Tsang, D. C. W.; Lee, K. B.; Ok, Y. S., Gasification biochar from biowaste (food waste and wood waste) for effective CO_2 adsorption. *Journal of Hazardous Materials* **2020**, *391*, 121147.
3. Kim, M.-J.; Choi, S. W.; Kim, H.; Mun, S.; Lee, K. B., Simple synthesis of spent coffee ground-based microporous carbons using K_2CO_3 as an activation agent and their application to CO_2 capture. *Chemical Engineering Journal* **2020**, *397*, 125404.
4. Wu, D.; Yang, Y.; Liu, J.; Zheng, Y., Plasma-modified N/O-doped porous carbon for CO_2 capture: An experimental and theoretical study. *Energy & Fuels* **2020**, *34*, (5), 6077-6084.
5. Sriram, G.; S, S.; Kurkuri, M.; Hegde, G., Efficient CO_2 adsorption using mesoporous carbons from biowastes. *Materials Research Express* **2019**, *7*, (1), 015605.
6. Quan, C.; Su, R.; Gao, N., Preparation of activated biomass carbon from pine sawdust for supercapacitor and CO_2 capture. *International Journal of Energy Research* **2020**, *44*, (6), 4335-4351.
7. Li, J.; Michalkiewicz, B.; Min, J.; Ma, C.; Chen, X.; Gong, J.; Mijowska, E.; Tang, T., Selective preparation of biomass-derived porous carbon with controllable pore sizes toward highly efficient CO_2 capture. *Chemical Engineering Journal* **2019**, *360*, 250-259.
8. Choi, S. W.; Tang, J.; Pol, V. G.; Lee, K. B., Pollen-derived porous carbon by KOH activation: Effect of physicochemical structure on CO_2 adsorption. *Journal of CO_2 Utilization* **2019**, *29*, 146-155.
9. Huang, G.; Wu, X.; Hou, Y.; Cai, J., Sustainable porous carbons from garlic peel biowaste and KOH activation with an excellent CO_2 adsorption performance. *Biomass Conversion & Biorefinery* **2020**, *10*, (2), 267-276.
10. Yuan, H.; Chen, J.; Li, D.; Chen, H.; Chen, Y., 5 Ultramicropore-rich renewable porous carbon from biomass tar with excellent adsorption capacity and selectivity for CO_2 capture. *Chemical Engineering Journal* **2019**, *373*, 171-178.
11. Li, D.; Chen, J.; Fan, Y.; Deng, L.; Shan, R.; Chen, H.; Yuan, H.; Chen, Y., Biomass-tar-enabled nitrogen-doped highly ultramicroporous carbon as an efficient absorbent for CO_2 capture. *Energy & Fuels* **2019**, *33*, (9), 8927-8936.
12. Ma, X.; Li, L.; Zeng, Z.; Chen, R.; Wang, C.; Zhou, K.; Li, H., Experimental and theoretical demonstration of the relative effects of O-doping and N-doping in porous carbons for CO_2 capture. *Applied Surface Science* **2019**, *481*, 1139-1147.
13. Sivadas, D. L.; Damodaran, A.; Raghavan, R., Microporous carbon monolith and fiber from freeze-dried banana stems for high efficiency carbon dioxide adsorption. *ACS Sustainable Chemistry & Engineering* **2019**, *7*, (15), 12807-12816.
14. Sun, H.; Yang, B.; Li, A., Biomass derived porous carbon for efficient capture of carbon dioxide, organic contaminants and volatile iodine with exceptionally high uptake. *Chemical Engineering Journal* **2019**, *372*, 65-73.

15. Gargiulo, V.; Gomis-Berenguer, A.; Giudicianni, P.; Ania, C. O.; Ragucci, R.; Alfè, M., Assessing the potential of biochars prepared by steam-assisted slow pyrolysis for CO_2 adsorption and separation. *Energy & Fuels: An American Chemical Society Journal* **2018**, *32*, (10), 10218-10227.
16. Xu, J.; Shi, J.; Cui, H.; Yan, N.; Liu, Y., Preparation of nitrogen doped carbon from tree leaves as efficient CO_2 adsorbent. *Chemical Physics Letters* **2018**, *711*, 107-112.
17. Shen, F.; Wang, Y.; Li, L.; Zhang, K.; Smith, R. L.; Qi, X., Porous carbonaceous materials from hydrothermal carbonization and KOH activation of corn stover for highly efficient CO_2 capture. *Chemical Engineering Communications* **2018**, *205*, (4), 423-431.
18. Singh, G.; Kim, I. Y.; Lakhi, K. S.; Srivastava, P.; Naidu, R.; Vinu, A., Single step synthesis of activated bio-carbons with a high surface area and their excellent CO_2 adsorption capacity. *Carbon* **2017**, *116*, 448-455.
19. Du, J.; Yu, Y.; Lv, H.; Chen, C.; Zhang, J.; Chen, A., Cauliflower-derived porous carbon without activation for electrochemical capacitor and CO_2 capture applications. *Journal of Nanoparticle Research* **2018**, *20*, (15), https://doi.org/10.1007/s11051-017-4109-y.
20. Wu, X.-x.; Zhang, C.-y.; Tian, Z.-w.; Cai, J.-j., Large-surface-area carbons derived from lotus stem waste for efficient CO_2 capture. *New Carbon Materials* **2018**, *33*, (3), 252-261.
21. Hirst, E. A.; Taylor, A.; Mokaya, R., A simple flash carbonization route for conversion of biomass to porous carbons with high CO_2 storage capacity. *Journal of Materials Chemistry A* **2018**, *6*, (26), 12393-12403.
22. Manyà, J. J.; González, B.; Azuara, M.; Arner, G., Ultra-microporous adsorbents prepared from vine shoots-derived biochar with high CO_2 uptake and CO_2/N_2 selectivity. *Chemical Engineering Journal* **2018**, *345*, 631-639.
23. Serafin, J.; Narkiewicz, U.; Morawski, A. W.; Wróbel, R. J.; Michalkiewicz, B., Highly microporous activated carbons from biomass for CO_2 capture and effective micropores at different conditions. *Journal of CO_2 Utilization* **2017**, *18*, 73-79.
24. Coromina, H. M.; Walsh, D. A.; Mokaya, R., Biomass-derived activated carbon with simultaneously enhanced CO_2 uptake for both pre and post combustion capture applications. *Journal of Materials Chemistry A* **2016**, *4*, (1), 280-289.
25. Parshetti, G. K.; Chowdhury, S.; Balasubramanian, R., Biomass derived low-cost microporous adsorbents for efficient CO_2 capture. *Fuel* **2015**, *148*, 246-254.
26. Zhang, C.; Song, W.; Ma, Q.; Xie, L.; Zhang, X.; Guo, H., Enhancement of CO_2 capture on biomass-based carbon from black locust by KOH activation and ammonia modification. *Energy & Fuels* **2016**, *30*, (5), 4181-4190.
27. Fiuza- Jr, R. A.; Andrade, R. C.; Andrade, H. M. C., CO_2 capture on KOH-activated carbons derived from yellow mombin fruit stones. *Journal of Environmental Chemical Engineering* **2016**, *4*, (4), 4229-4236.
28. Alabadi, A.; Razzaque, S.; Yang, Y.; Chen, S.; Tan, B., Highly porous activated carbon materials from carbonized biomass with high CO_2 capturing capacity. *Chemical Engineering Journal* **2015**, *281*, 606-612.
29. Li, D.; Ma, T.; Zhang, R.; Tian, Y.; Qiao, Y., Preparation of porous carbons with high low-pressure CO_2 uptake by KOH activation of rice husk char. *Fuel* **2015**, *139*, 68-70.

30. Li, D.; Tian, Y.; Li, L.; Li, J.; Zhang, H., Production of highly microporous carbons with large CO_2 uptakes at atmospheric pressure by KOH activation of peanut shell char. *Journal of Porous Materials* **2015**, *22*, (6), 1581-1588.
31. Song, J.; Shen, W.; Wang, J.; Fan, W., Superior carbon-based CO_2 adsorbents prepared from poplar anthers. *Carbon* **2014**, *69*, 255-263.
32. Deng, S.; Wei, H.; Chen, T.; Wang, B.; Huang, J.; Yu, G., Superior CO_2 adsorption on pine nut shell-derived activated carbons and the effective micropores at different temperatures. *Chemical Engineering Journal* **2014**, *253*, 46-54.
33. Bae, J.-S.; Su, S., Macadamia nut shell-derived carbon composites for post combustion CO_2 capture. *International Journal of Greenhouse Gas Control* **2013**, *19*, 174-182.
34. Zhu, M. Y.; Cai, W. Q.; Verpoort, F.; Zhou, J. B., Preparation of pineapple waste-derived porous carbons with enhanced CO_2 capture performance by hydrothermal carbonation-alkali metal oxalates assisted thermal activation process. *Chemical Engineering Research & Design* **2019**, *146*, 130-140.
35. Cui, H.; Xu, J.; Shi, J.; Yan, N.; Liu, Y.; Zhang, S., Zinc nitrate as an activation agent for the synthesis of nitrogen-doped porous carbon and its application in CO_2 adsorption. *Energy & Fuels* **2020**, *34*, (5), 6069-6076.
36. Xu, J.; Cui, H.; Shi, J.; Yan, N.; Liu, Y.; Li, D., Agar-derived nitrogen-doped porous carbon for CO_2 adsorption. *ChemistrySelect* **2018**, *3*, (39), 10977-10982.
37. Liu, S. F.; Ma, R.; Hu, X.; Wang, L. L.; Wang, X. Y.; Radosz, M.; Fan, M. H., CO_2 adsorption on hazelnut-shell-derived nitrogen-doped porous carbons synthesized by single-step sodium amide activation. *Industrial & Engineering Chemistry Research* **2020**, *59*, (15), 7046-7053.
38. Yang, Z.; Zhang, G.; Guo, X.; Xu, Y., Designing a novel N-doped adsorbent with ultrahigh selectivity for CO_2: Waste biomass pyrolysis and two-step activation. *Biomass Conversion & Biorefinery* **2020**. https://doi.org/10.1007/s13399-020-00633-0.
39. Xu, Y.; Yang, Z.; Zhang, G.; Zhao, P., Excellent CO_2 adsorption performance of nitrogen-doped waste biocarbon prepared with different activators. *Journal of Cleaner Production* **2020**, *264*.
40. Yang, Z.; Zhang, G.; Xu, Y.; Zhao, P., One step N-doping and activation of biomass carbon at low temperature through $NaNH_2$: An effective approach to CO_2 adsorbents. *Journal of CO_2 Utilization* **2019**, *33*, 320-329.
41. Quan, C.; Jia, X.; Gao, N., Nitrogen-doping activated biomass carbon from tea seed shell for CO_2 capture and supercapacitor. *International Journal of Energy Research* **2019**, *44*, (2), 1218-1232.
42. Rao, L.; Liu, S.; Wang, L.; Ma, C.; Wu, J.; An, L.; Hu, X., N-doped porous carbons from low-temperature and single-step sodium amide activation of carbonized water chestnut shell with excellent CO_2 capture performance. *Chemical Engineering Journal* **2019**, *359*, 428-435.
43. Ma, R.; Hao, J.; Chang, G.; Wang, Y.; Guo, Q., Nitrogen-doping microporous adsorbents prepared from palm kernel with excellent CO_2 capture property. *Canadian Journal of Chemical Engineering* **2019**, *98*, (2), 503-512.
44. Wei, H.; Chen, J.; Fu, N.; Chen, H.; Lin, H.; Han, S., Biomass-derived nitrogen-doped porous carbon with superior capacitive performance and high CO_2 capture capacity. *Electrochimica Acta* **2018**, *266*, 161-169.

45. Yue, L.; Xia, Q.; Wang, L.; Wang, L.; DaCosta, H.; Yang, J.; Hu, X., CO_2 adsorption at nitrogen-doped carbons prepared by K_2CO_3 activation of urea-modified coconut shell. *Journal of Colloid & Interface Science* **2018**, *511*, 259-267.

46. Chen, J.; Yang, J.; Hu, G. S.; Hu, X.; Li, Z. M.; Shen, S. W.; Radosz, M.; Fan, M. H., Enhanced CO_2 capture capacity of nitrogen-doped biomass-derived porous carbons. *ACS Sustainable Chemistry & Engineering* **2016**, *4*, (3), 1439-1445.

47. Yang, M.; Guo, L.; Hu, G.; Hu, X.; Xu, L.; Chen, J.; Dai, W.; Fan, M., Highly cost-effective nitrogen-doped porous coconut shell-based CO_2 sorbent synthesized by combining ammoxidation with KOH activation. *Environmental Science & Technology* **2015**, *49*, (11), 7063-7070.

48. Boujibar, O.; Souikny, A.; Ghamouss, F.; Achak, O.; Dahbi, M.; Chafik, T., CO_2 capture using N-containing nanoporous activated carbon obtained from argan fruit shells. *Journal of Environmental Chemical Engineering* **2018**, *6*, (2), 1995-2002.

49. Wei, H.; Chen, H.; Fu, N.; Chen, J.; Lan, G.; Qian, W.; Liu, Y.; Lin, H.; Han, S., Excellent electrochemical properties and large CO_2 capture of nitrogen-doped activated porous carbon synthesised from waste longan shells. *Electrochimica Acta* **2017**, *231*, 403-411.

50. Chithra, A.; Wilson, P.; Rajeev, R.; Prabhakaran, K., Nitrogen-doped microporous carbon with high CO_2 sorption by KOH activation of black gram. *Materials Research Express* **2018**, *5*, (11).

51. Yang, Z.; Guo, X.; Zhang, G.; Xu, Y., One-pot synthesis of high N-doped porous carbons derived from a N-rich oil palm biomass residue in low temperature for CO_2 capture. *International Journal of Energy Research* **2020**, *44*, (6), 4875-4887.

52. Li, Y.; Wang, S.; Wang, B.; Wang, Y.; Wei, J., Sustainable biomass glucose-derived porous carbon spheres with high nitrogen doping: As a promising adsorbent for $CO_2/CH_4/N_2$ adsorptive separation. *Nanomaterials* **2020**, *10*, (1), 174.

53. Chang, B.; Shi, W.; Yin, H.; Zhang, S.; Yang, B., Poplar catkin-derived self-templated synthesis of N-doped hierarchical porous carbon microtubes for effective CO_2 capture. *Chemical Engineering Journal* **2019**, *358*, 1507-1518.

54. Rao, L.; Ma, R.; Liu, S.; Wang, L.; Wu, Z.; Yang, J.; Hu, X., Nitrogen enriched porous carbons from d-glucose with excellent CO_2 capture performance. *Chemical Engineering Journal* **2019**, *362*, 794-801.

55. Rehman, A.; Park, S.-J., Tunable nitrogen-doped microporous carbons: Delineating the role of optimum pore size for enhanced CO_2 adsorption. *Chemical Engineering Journal* **2019**, *362*, 731-742.

56. Yue, L.; Rao, L.; Wang, L.; An, L.; Hou, C.; Ma, C.; DaCosta, H.; Hu, X., Efficient CO_2 Adsorption on Nitrogen-Doped porous carbons Derived from d-glucose. *Energy & Fuels* **2018**, *32*, (6), 6955-6963.

57. Park, S.; Choi, M. S.; Park, H. S., Nitrogen-doped nanoporous carbons derived from lignin for high CO_2 capacity. *Carbon Letters* **2019**, *29*, (3), 289-296.

58. Demir, M.; Tessema, T.-D.; Farghaly, A. A.; Nyankson, E.; Saraswat, S. K.; Aksoy, B.; Islamoglu, T.; Collinson, M. M.; El-Kaderi, H. M.; Gupta, R. B., Lignin-derived heteroatom-doped porous carbons for supercapacitor and CO_2 capture applications. *International Journal of Energy Research* **2018**, *42*, (8), 2686-2700.

59. Saha, D.; Van Bramer, S. E.; Orkoulas, G.; Ho, H.-C.; Chen, J.; Henley, D. K., CO_2 capture in lignin-derived and nitrogen-doped hierarchical porous carbons. *Carbon* **2017**, *121*, 257-266.
60. Han, J.; Zhang, L.; Zhao, B.; Qin, L.; Wang, Y.; Xing, F., The N-doped activated carbon derived from sugarcane bagasse for CO_2 adsorption. *Industrial Crops & Products* **2019**, *128*, 290-297.
61. Rao, L.; Yue, L.; Wang, L.; Wu, Z.; Ma, C.; An, L.; Hu, X., Low-temperature and single-step synthesis of N-doped porous carbons with a high CO_2 adsorption performance by sodium amide activation. *Energy & Fuels* **2018**, *32*, (10), 10830-10837.
62. Wang, L.; Rao, L.; Xia, B.; Wang, L.; Yue, L.; Liang, Y.; DaCosta, H.; Hu, X., Highly efficient CO_2 adsorption by nitrogen-doped porous carbons synthesized with low-temperature sodium amide activation. *Carbon* **2018**, *130*, 31-40.
63. Singh, M. G.; Lakhi, K. S.; Park, D.-H.; Srivastava, P.; Naidu, R.; Vinu, A., Facile one-pot synthesis of activated porous biocarbons with a high nitrogen content for CO_2 capture. *ChemNanoMat* **2018**, *4*, (3), 281-290.
64. Gao, A.; Guo, N.; Yan, M.; Li, M.; Wang, F.; Yang, R., Hierarchical porous carbon activated by $CaCO_3$ from pigskin collagen for CO_2 and H_2 adsorption. *Microporous & Mesoporous Materials* **2018**, *260*, 172-179.
65. Li, D.; Zhou, J.; Zhang, Z.; Li, L.; Tian, Y.; Lu, Y.; Qiao, Y.; Li, J.; Wen, L., Improving low-pressure CO_2 capture performance of N-doped active carbons by adjusting flow rate of protective gas during alkali activation. *Carbon* **2017**, *114*, 496-503.
66. Yue, L.; Rao, L.; Wang, L.; Wang, L.; Wu, J.; Hu, X.; DaCosta, H.; Yang, J.; Fan, M., Efficient CO_2 capture by nitrogen-doped biocarbons derived from rotten strawberries. *Industrial & Engineering Chemistry Research* **2017**, *56*, (47), 14115-14122.
67. Rana, M.; Subramani, K.; Sathish, M.; Gautam, U. K., Soya derived heteroatom doped carbon as a promising platform for oxygen reduction, supercapacitor and CO_2 capture. *Carbon* **2017**, *114*, 679-689.
68. Singh, G.; Kim, I. Y.; Lakhi, K. S.; Joseph, S.; Srivastava, P.; Naidu, R.; Vinu, A., Heteroatom functionalized activated porous biocarbons and their excellent performance for CO_2 capture at high pressure. *Journal of Materials Chemistry A* **2017**, *5*, (40), 21196-21204.
69. Li, Y.; Xu, R.; Wang, X.; Wang, B.; Cao, J.; Yang, J.; Wei, J., Waste wool derived nitrogen-doped hierarchical porous carbon for selective CO_2 capture. *RSC Advances* **2018**, *8*, (35), 19818-19826.
70. Zhu, B.; Qiu, K.; Shang, C.; Guo, Z., Naturally derived porous carbon with selective metal- and/or nitrogen-doping for efficient CO_2 capture and oxygen reduction. *Journal of Materials Chemistry A* **2015**, *3*, (9), 5212-5222.
71. Liu, S. H.; Huang, Y. Y., Valorization of coffee grounds to biochar-derived adsorbents for CO_2 adsorption. *Journal of Cleaner Production* **2018**, *175*, 354-360.
72. Wei, T.; Zhang, Q.; Wei, X.; Gao, Y.; Li, H., A facile and low-cost route to heteroatom doped porous carbon derived from Broussonetia papyrifera Bark with excellent supercapacitance and CO_2 capture performance. *Scientific Rep*orts **2016**, *6*, 22646.
73. Arami-Niya, A.; Rufford, T. E.; Zhu, Z.; Carbon, N.-D., Foams synthesized from banana peel and zinc complex template for adsorption of CO_2, CH_4, and N_2. *Energy & Fuels* **2016**, *30*, (9), 7298-7309.

74. Boyjoo, Y.; Cheng, Y.; Zhong, H.; Tian, H.; Pan, J.; Pareek, V. K.; Jiang, S. P.; Lamonier, J.-F.; Jaroniec, M.; Liu, J., From waste Coca Cola® to activated carbons with impressive capabilities for CO_2 adsorption and supercapacitors. *Carbon* **2017**, *116*, 490-499.
75. Zhao, Z.-Q.; Xiao, P.-W.; Zhao, L.; Liu, Y.; Han, B.-H., Human hair-derived nitrogen and sulfur co-doped porous carbon materials for gas adsorption. *RSC Advances* **2015**, *5*, (90), 73980-73988.
76. Querejeta, N.; Gil, M. V.; Pevida, C.; Centeno, T. A., Standing out the key role of ultramicroporosity to tailor biomass-derived carbons for CO_2 capture. *Journal of CO_2 Utilization* **2018**, *26*, 1-7.
77. Li, J.; Pan, L.; Suvarna, M.; Tong, Y. W.; Wang, X., Fuel properties of hydrochar and pyrochar: Prediction and exploration with machine learning. *Applied Energy* **2020**, *269*, 115166.